

Advanced RPE PPLN Waveguide Applications: Beyond SHG and Uniform QPM Gratings

Carsten Langrock and Martin M. Fejer

Edward L. Ginzton Laboratory, Stanford University, Stanford, CA 94305

Apodization of linearly chirped QPM gratings in periodically-poled lithium niobate

For second harmonic generation (SHG), it has been shown that the transfer function of a quasi-phasematched (QPM) device is directly related to the Fourier transform of its grating function [1]. For a uniform grating of finite length, this results in a sinc^2 response of the SH signal as a function of fundamental wavelength with its center determined by the material dispersion and QPM period, and its width (SH bandwidth) given by the length of the grating; the longer the grating, the narrower the SH bandwidth.

One way to achieve large bandwidths is to shorten the grating length. While this does indeed increase the bandwidth, it also reduces the effective interaction length, greatly reducing the maximum achievable conversion efficiency; the efficiency is proportional to the square of the interaction length in guided wave devices. For waveguide-based QPM devices, a better method of increasing the bandwidth is based on variation of the QPM period as a function of position along the propagation direction inside the waveguide. Besides engineering the bandwidth of a device, its phase response can also be altered which has been successfully used to temporally compress the SH output using a chirped input pulse [2]. So far, less attention has been paid to engineering of the amplitude response.

Figure 1 depicts the theoretical SH transfer function of a linearly chirped QPM grating with 50-nm bandwidth centered around 1545 nm. One notices that the magnitude within the “passband” of the device exhibits significant ripples, indicating large variations in conversion efficiency as a function of fundamental wavelength. These rip-

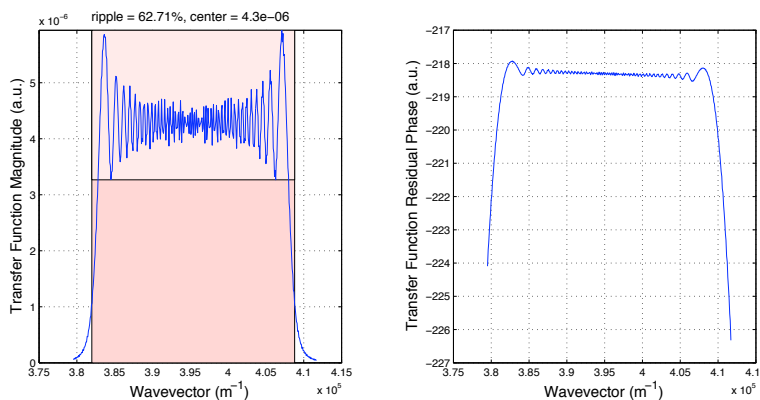


Figure 1. Theoretical amplitude and phase response of a linearly chirped QPM grating with 50-nm bandwidth centered around 1545 nm. The ripple in the “passband” is clearly visible and undesirable for most applications. The residual phase is flat after subtraction of the quadratic component.

ples might be undesired for some applications and methods for their reduction are outlined in this report.

The origin of the above shown ripples in the “passband” of the transfer function are easily identified. They are caused by the “hard edges” formed by the interfaces between regions without and with QPM structures found at the beginning and end of the grating. At these interfaces, the nonlinearity experienced by the propagating fundamental wave jumps from virtually zero to a large value and vice versa. Discontinuities like these are well known to cause “ringing” in analog as well as digital filters and have been overcome in those instances by tapering or apodizing the action of the device under test as a function of the free parameter, e.g. time or frequency.

Our group has investigated several different methods for the tapering of the local nonlinearity. These apodization methods are not only useful for chirped gratings, but proved useful for the significant suppression of the sidelobes in uniform gratings required by some telecommunication applications to avoid crosstalk between closely spaced

signals [3]. The various apodization methods investigated are described in [3] and won't be repeated here for brevity.

Based on simulations, we designed, fabricated, and characterized reverse-proton-exchanged (RPE) waveguide devices on periodically-poled lithium niobate (PPLN) substrates implementing various apodization target functions of varying lengths as well as 25-nm and 50-nm wide passbands. We found that apodization lengths beyond 20% of the total QPM length do not further increase the flatness of the passband due to limitations imposed by random duty cycle fluctuations as well as waveguide nonuniformities. While the experimentally achieved ripple reduction is significant (see Figure 2), we are convinced that further improvements can be achieved by tighter duty cycle and waveguide uniformity control.

These devices have already been used for high-sensitivity autocorrelation and frequency-resolved optical gating (FROG) measurements of ultra-short optical pulses in the telecommunication C-band [4]. Experiments conducted at the Lawrence Livermore National Laboratory on temporal magnification of ultra-short pulse sequences via the time-lens method [5] are currently underway and are expected to result in sensitivity improvements in excess of two orders of magnitude as compared to bulk PPLN devices.

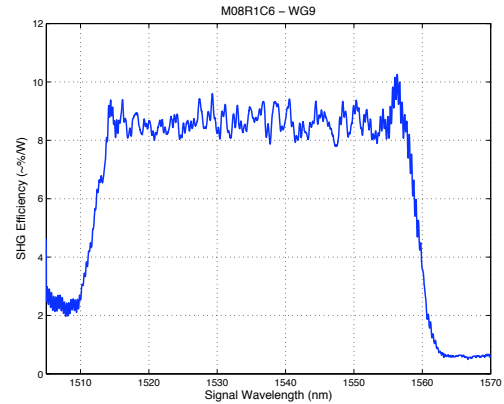


Figure 2. Experimental results showing the conversion efficiency of an apodized QPM grating with 50-nm wide bandwidth.

Guided-wave singly-resonant CW PPLN RPE fiber-loop ring OPO

The device presented here represents a fully-integrated singly-resonant CW ring optical parametric oscillator (OPO) using an RPE PPLN waveguide. Pump coupling as well as resonant feedback is provided via single-mode optical fibers pigtailed to the waveguide device. The OPO can be tuned over the parametric gain bandwidth (> 60 nm around the 1558 nm center wavelength) via a frequency selective element inside the feedback loop. While there are well established sources available for C-band wavelengths, the device concept presented here can easily be expanded to other wavelengths of interest.

A schematic of our experimental setup can be seen in Figure 3a. Light from an external cavity tunable diode laser (ECDL) running at 779 nm is coupled into the RPE PPLN waveguide device. The generated C-band signals are then coupled into a single-mode fiber at the output of the device via an on-chip directional coupler as shown in Figure 3b. After passing a frequency selective element (here, a 1563 nm reflecting fiber Bragg grating (FBG) attached to a circulator), they are fed back into the waveguide's input via an identical directional coupler. Light not reflected by the FBG is split and monitored using a grating-based (HP 86142A) and an interferometric (Advantest Q8347) optical spectrum analyzer (OSA).

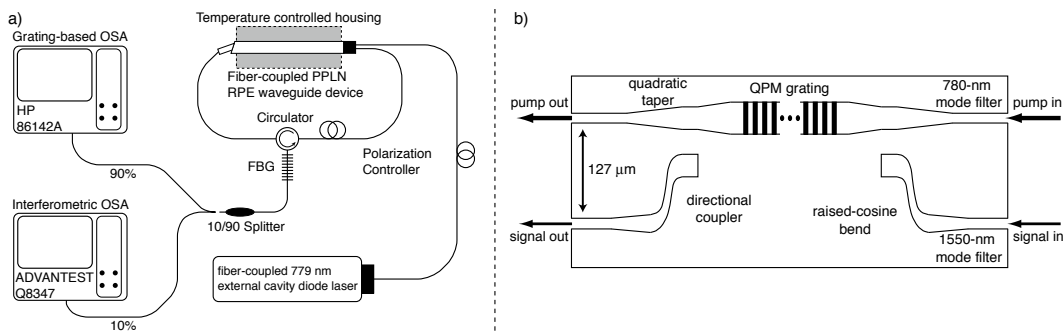


Figure 3. a) experimental setup; b) schematic of PPLN waveguide device.

The initial characterization of the device was performed via difference frequency generation (DFG) by opening the ring cavity and injecting light from a C-band ECDL and monitoring the amplified output signal as well as the generated difference frequency as a function of crystal temperature and pump power. The experimental results shown in Figure 4 are in good agreement with theoretical predictions and demonstrate the large parametric gain bandwidth (> 60 nm) of this device.

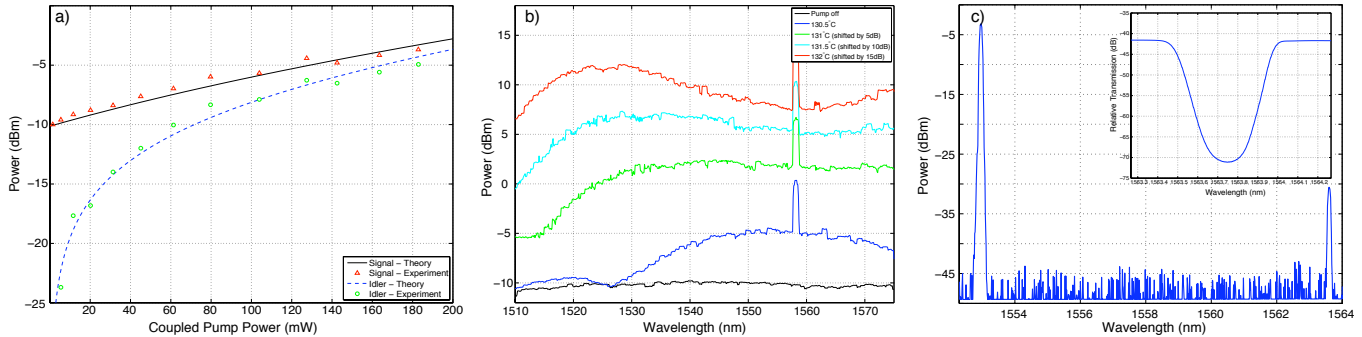


Figure 4. a) theoretical and experimental results of parametric gain characterization via DFG.; b) parametric gain bandwidth as a function of crystal temperature; the spike at 1558 nm is due to the 779-nm pump appearing in second order in the grating-based OSA; c) HP-86142A OSA trace showing both resonated signal and out-coupled idler (inset shows the FBG's transmission spectrum).

After closing the ring cavity, singly-resonant oscillation started at a coupled pump power of approximately 200 mW. This threshold is set by loop losses such as the circulator, sub-optimal waveguide-to-fiber coupling, as well as waveguide propagation losses and can be significantly reduced in further optimized devices. We observed single peaks at 1563 nm and 1553 nm on the interferometric OSA. Due to this OSA's resolution bandwidth limit of 7 pm, we cannot claim single axial mode operation, even though past experimental results have shown that ring OPOs frequently run on a single axial mode [6].

Tuning of the oscillation frequency over the parametric gain bandwidth provided by the QPM structure can be achieved by replacing the fixed FBG with a tunable one. The doubly-resonant (DRO) case has also been investigated by replacing the frequency selective element with a power splitter. While the DRO threshold is significantly lower (~ 30 mW), stable DRO operation has not been achieved to this point. Separation of the conjugate C-band signals and independent phase control would have to be implemented to improve DRO operation.

References

1. G. Imeshev, M. A. Arbore, M. M. Fejer, A. Galvanauskas, M. Fermann, and D. Harter, "Ultrashort-Pulse Second Harmonic Generation with Longitudinally Nonuniform Gratings: Pulse Compression and Shaping", *J. Opt. Sci. Am. B.* 17, pp. 304-318 (February 2000)
2. A. M. Schober, G. Imeshev, M. M. Fejer, "Tunable-chirp pulse compression in quasi-phase-matched second-harmonic generation", *Opt. Lett.* 27, pp. 1129-31 (July 2002)
3. Jie Huang, X. P. Xie, Carsten Langrock, R. V. Roussev, D. S. Hum, and M. M. Fejer, "Amplitude modulation and apodization of quasi-phase-matched interactions", *Opt. Lett.*, No. 5 Vol. 31 pp. 604-606 (March 2006)
4. H. Miao, A. M. Weiner, S. Yang, C. Langrock, R. V. Roussev, M. M. Fejer, "Ultrasensitive Second-Harmonic Generation Frequency-Resolved Optical Gating Using a Fiber-Pigtailed Aperiodically Poled Lithium Niobate Waveguide at 1.55 μm ," 15th International Conference on Ultrafast Phenomena, WC2 (2006)
5. C. V. Bennett and B. H. Kolner, "Upconversion time microscope demonstrating 103x magnification of femto-second waveforms", *Opt. Lett.*, Vol. 24, No. 11, pp. 783 - 5 (June 1999)
6. W. R. Bosenberg, A. Drobshoff, J. I. Alexander, L. E. Myers, and R. L. Byer, "93% pump depletion, 3.5-W continuous-wave, singly resonant optical parametric oscillator," *Opt. Lett.*, vol. 21, no. 17, pp. 1336 - 8 (September 1996)